Adaptive trajectory tracking for quadrotor MAVs in presence of parameter uncertainties and external disturbances

Gianluca Antonelli, Filippo Arrichiello, Stefano Chiaverini, Paolo Robuffo Giordano

▶ **To cite this version:**

HAL Id: hal-00910776

https://hal.inria.fr/hal-00910776

Submitted on 10 Dec 2013

Adaptive trajectory tracking for quadrotor MAVs in presence of parameter uncertainties and external disturbances

Gianluca Antonelli[†], Filippo Arrichiello[†], Stefano Chiaverini[†], Paolo Robuffo Giordano[‡]

Abstract— The paper presents an adaptive trajectory tracking control strategy for quadrotor Micro Aerial Vehicles. The proposed approach, while keeping the typical assumption of an orientation dynamics faster than the translational one, removes that of absence of external disturbances and of perfect symmetry of the vehicle. In particular, the trajectory tracking control law is made adaptive with respect to the presence of external forces and moments, and to the uncertainty of dynamic parameters as the position of the center of mass of the vehicle. A stability analysis as well as numerical simulations are provided to support the control design.

I. INTRODUCTION

Over the last years, the use of Micro Aerial Vehicles (MAVs) as robotic platforms has witnessed the growing attention of the robotics community. Typical envisioned tasks for MAVs involve traffic surveillance, monitoring of air pollution, area mapping, inspection of collapsed building or dangerous sites, and agricultural applications such as pesticide spraying. Among the different advantages offered by MAVs, their capabilities to take off and land in limited spaces and to hover above targets are of crucial importance.

Several research groups have recently focused their activities on the development of high-performance flight control and motion planning algorithms for single and/or multiple MAVs; for the experimental validation, they usually exploit suitable indoor facilities equipped with an external visual tracking system for fast and accurate state estimation [1], [2]. At the same time, other research groups have addressed the problem of estimating the MAV position/orientation online by only relying on onboard sensing (usually, cameras and IMU) and (limited) computation capabilities, see [3], [4], [5], [6]. Furthermore, the potentiality of MAVs has been demonstrated in cooperative transportation tasks [7], aerial grasping of moving objects [8], and in complex missions involving distributed sensing and coordination among several MAVs [9], [10], [11].

For all the applications involving MAVs, ensuring a good and robust performance of the underlying flight controller represents a fundamental requirement. The works in [12], [13] offer an interesting introduction to the theory involved, as well as some experimental results concerning *quadrotors vehicles*, i.e., MAVs equipped with four thrusters aligned in the same direction — a nowadays widespread solution in research labs. Quadrotor MAVs are, as well-known, underactuated mechanical systems (6 Degrees-Of-Freedom (DOFs) vs. 4 control inputs). A common strategy to handle the quadrotor motion is to only control its 3D position and yaw angle, since these are flat outputs for the system [14]. To counteract external disturbances such as, e.g., the wind, integral-based

actions may be implemented; however, without a proper knowledge of the dynamics under investigation, the use of adaptive or integral control actions may eventually feed the closed loop system with an additional *disturbance* rather than reducing it, see, e.g., [15]. At the best of our knowledge, the only adaptive control for MAVs is proposed in [16]; in that solution, the mathematical model is rewritten in order to make clear its linear dependency with respect to the sole center of gravity position, which is then successively used in a feedback linearization approach.

This paper presents an adaptive control technique for trajectory tracking of quadrotors that removes the assumption of known dynamic parameters (in particular the position of the center of mass) and considers the presence of constant external forces/moments. With respect to [16], this paper proposes a different adaptive approach, it explicitly considers the external disturbances in the stability analysis, it isolates a minimal set of parameters to be identified, and it finally takes into account the effect of a wrong projection from desired forces to thrusters velocities due to a poor barycenter estimation. A detailed mathematical analysis and numerical simulations show the efficacy of the proposed approach. The proposed adaptive controller would consistently improve the reliability/robustness of MAVs operations, especially in outdoor environments (wind) or in applications involving picking and releasing of small loads (barycenter shift).

II. MODELING

A. Kinematics

A rigid body is completely described by its position and orientation with respect to a reference frame $\Sigma_i, O - \boldsymbol{xyz}$ assumed earth-fixed and inertial. Let $\boldsymbol{\eta}_1 \in \mathbb{R}^3$

$$\boldsymbol{\eta}_1 = \begin{bmatrix} x & y & z \end{bmatrix}^{\mathrm{T}}$$

be the vector of the body position coordinates in an earth-fixed reference frame. The vector $\dot{\boldsymbol{\eta}}_1$ is the corresponding time derivative (expressed in the earth-fixed frame). If one defines $\boldsymbol{\nu}_1 = \begin{bmatrix} u & v & w \end{bmatrix}^{\mathrm{T}}$ as the linear velocity of the origin of the body-fixed frame $\Sigma_b, O_b - \boldsymbol{x}_b\boldsymbol{y}_b\boldsymbol{z}_b$ with respect to the origin of the earth-fixed frame, expressed in the body-fixed frame (from now on: body-fixed linear velocity), then the following relation between the defined linear velocities holds:

$$\boldsymbol{\nu}_1 = \boldsymbol{R}_I^B \dot{\boldsymbol{\eta}}_1, \tag{1}$$

where $\boldsymbol{R}_I^B$ is the rotation matrix expressing the transformation from the inertial frame to the body-fixed frame.

Define $\boldsymbol{\eta}_2 \in \mathbb{R}^3$ as

$$\boldsymbol{\eta}_2 = \begin{bmatrix} \phi & \theta & \psi \end{bmatrix}^{\mathrm{T}},$$

the set of body Euler-angle coordinates in a earth-fixed reference frame. Those are commonly named roll, pitch and yaw angles and correspond to the succesive elementary rotations around x, y and z in the fixed frame [17]. The vector $\dot{\boldsymbol{\eta}}_2$ is the corresponding time derivative (expressed in the inertial frame). Let define $\boldsymbol{\nu}_2 = \begin{bmatrix} p & q & r \end{bmatrix}^{\mathrm{T}}$ as the angular velocity of the body-fixed frame with respect to the earth-fixed frame expressed in the body-fixed frame (from now on: body-fixed angular velocity). The vector $\dot{\boldsymbol{\eta}}_2$ does not have a physical interpretation and it is related to the body-fixed angular velocity by a proper Jacobian matrix:

$$\boldsymbol{\nu}_2 = \boldsymbol{J}_{k,o}(\boldsymbol{\eta}_2)\dot{\boldsymbol{\eta}}_2. \qquad (2)$$
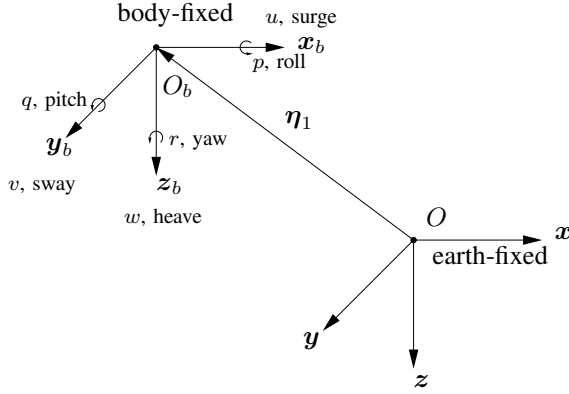
Figure 1 shows the defined frames and the elementary motions.

Fig. 1. Frames and elementary vehicle's motion

B. Dynamics

The rigid body dynamics of a quadrotor, in matrix form, is given by:

$$\boldsymbol{M}_{RB}\dot{\boldsymbol{\nu}} + \boldsymbol{C}_{RB}(\boldsymbol{\nu})\boldsymbol{\nu} + \boldsymbol{\tau}_{v,W} + \boldsymbol{g}_{RB}(\boldsymbol{R}_I^B) = \boldsymbol{\tau}_v, \qquad (3)$$

where $\boldsymbol{\tau}_v = \begin{bmatrix} \boldsymbol{\tau}_1^{\mathrm{T}} & \boldsymbol{\tau}_2^{\mathrm{T}} \end{bmatrix}^{\mathrm{T}}$, the vector $\boldsymbol{\tau}_1 = \begin{bmatrix} X & Y & Z \end{bmatrix}^{\mathrm{T}}$ collects the linear forces acting on the rigid body expressed in a body-fixed frame, while $\boldsymbol{\tau}_2 = \begin{bmatrix} K & M & N \end{bmatrix}^{\mathrm{T}}$ collects the moments acting on the rigid body expressed in a body-fixed frame.

The matrix $\boldsymbol{M}_{RB}$ is constant, symmetric and positive definite, i.e., $\dot{\boldsymbol{M}}_{RB} = \boldsymbol{O}$, $\boldsymbol{M}_{RB} = \boldsymbol{M}_{RB}^{\mathrm{T}} > \boldsymbol{O}$. Its unique parametrization takes the form:

$$\boldsymbol{M}_{RB} = \begin{bmatrix} m\boldsymbol{I}_3 & -m\boldsymbol{S}(\boldsymbol{r}_C^b) \\ m\boldsymbol{S}(\boldsymbol{r}_C^b) & \boldsymbol{I}_{O_b} \end{bmatrix},$$

where $\boldsymbol{I}_3$ is the (3×3) identity matrix, $\boldsymbol{r}_C^b \in \mathbb{R}^3$ is the center-of-mass position expressed in body-fixed frame and $\boldsymbol{I}_{O_b}$ is the inertia tensor expressed in the body-fixed frame.

Notice that (3) can be simplified if the origin of the body-fixed frame is chosen coincident with the central frame, i.e., $\boldsymbol{r}_C^b = \boldsymbol{0}$ and $\boldsymbol{I}_{O_b}$ is a diagonal matrix.

The gravity force, acting in the center of mass $\boldsymbol{r}_C^b$, is represented in body-fixed frame by:

$$\boldsymbol{g}_{RB}(\boldsymbol{R}_I^B) = \begin{bmatrix} m\boldsymbol{R}_I^B \boldsymbol{g}^I \\ \boldsymbol{0}_{3\times 1} \end{bmatrix}$$

where $\boldsymbol{g}^I = \begin{bmatrix} 0 & 0 & 9.81 \end{bmatrix}^{\mathrm{T}}$.

The term $\boldsymbol{\tau}_{v,W} \in \mathbb{R}^6$ represents external disturbances such as the wind; its effect on the vehicle is modeled as a constant disturbance in the earth-fixed frame that is further projected onto the vehicle-fixed frame. To this purpose, let define as $\boldsymbol{\gamma}_{v,W} \in \mathbb{R}^6$ a vector of constant parameters; the current disturbance in the vehicle-fixed frame can be modelled as

$$\boldsymbol{\tau}_{v,W} = \boldsymbol{\Phi}_{v,W}(\boldsymbol{R}_B^I)\boldsymbol{\gamma}_{v,W} = \begin{bmatrix} \boldsymbol{R}_I^B & \boldsymbol{O}_{3\times 3} \\ \boldsymbol{O}_{3\times 3} & \boldsymbol{R}_I^B \end{bmatrix} \boldsymbol{\gamma}_{v,W} \qquad (4)$$

where the (6×6) regressor matrix $\boldsymbol{\Phi}_{v,W}$ simply expresses the force/moment coordinate transformation between the two frames.

It is possible to rewrite eq. (3) by exploiting the linearity in the parameters as:

$$\boldsymbol{\Phi}_v(\dot{\boldsymbol{\nu}}, \boldsymbol{\nu}, \boldsymbol{R}_I^B)\boldsymbol{\gamma}_v = \boldsymbol{\tau}_v \qquad (5)$$

where $\boldsymbol{\gamma}_v \in \mathbb{R}^{16}$ is the vector of the dynamic parameters collecting the mass (1 parameter), the first moment of inertia (3 parameters), the inertia tensor (6 parameters) and the 6 elements of the disturbance $\boldsymbol{\gamma}_{v,W}$. The same equation may be easily rewritten with respect to the variables expressed in the inertial frame $\boldsymbol{\eta}, \dot{\boldsymbol{\eta}}, \ddot{\boldsymbol{\eta}}$ following the guidelines of, e.g., [17]. In the following, the term $\boldsymbol{\Phi}_{xy} \in \mathbb{R}^{2\times 16}$ will denote the first two rows while $\boldsymbol{\phi}_z \in \mathbb{R}^{1\times 16}$ the third one of the regressor matrix expressed in the inertial frame. Following the guidelines of [18], well established in robotics [19], it is possible to further elaborate the regressor and classify the parameters among the sets: unidentifiable, identifiable alone and identifiable in linear combination. As an example, the body is affected by a vertical force caused by both the gravity and the wind; those effects can not be separated and the corresponding parameters will be identifiable in linear combination only. For sake of space, in this work the details are omitted; the controller tested in the following, in fact, will only consider the parameters that affect the steady state error.

C. Thrust

Quadrotors are equipped with 4 thrusters aligned along the body-fixed z axis with position $\boldsymbol{p}_{t,i}^b \in \mathbb{R}^3$, and each of them provide each a force and a moment according to

$$f_i = b\omega_{t,i}^2 \qquad \tau_{t,i} = d\omega_{t,i}^2 \qquad \text{for } i = 1, \dots, 4$$

where $\omega_{t,i}$ is the angular velocity of the ith rotor, b and d are the thrust and drag coefficients. Figure 2 reports the common motor position with relevant variables. Notice that the body-fixed frame is positioned in the *geometric* center of the vehicle, i.e., in the intersection between the two thrusters axes.
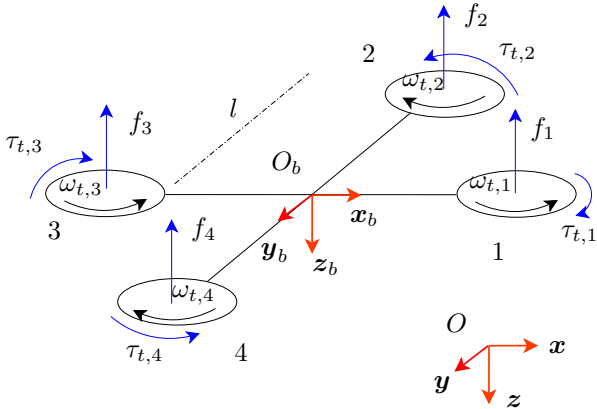
Fig. 2. Thrusters related variables

It holds

$$\boldsymbol{\tau}_1 = \begin{bmatrix} 0 & 0 & \sum_{i=1}^{4} f_i \end{bmatrix}^{\mathrm{T}}.$$

By initially assuming that the center of gravity is coincident with the geometric center of the quadrotor and with a proper numeration of the thrusters (the first is on the positive $\boldsymbol{x}_b$ axis and the numeration follows counter-clockwise looking from above), it holds:

$$\boldsymbol{\tau}_2 = \begin{bmatrix} l(f_2 - f_4) \\ l(f_1 - f_3) \\ -\tau_{t,1} + \tau_{t,2} - \tau_{t,3} + \tau_{t,4} \end{bmatrix}$$

Let us now consider a center of gravity not coincident with the origin of the body-fixed frame, i.e. $\boldsymbol{r}_C^b = \begin{bmatrix} r_{C,x} & r_{C,y} & r_{C,z} \end{bmatrix}^{\mathrm{T}} \neq \boldsymbol{0}^{\mathrm{T}}$. Due to the distributive property over the addition of the cross product, it is possible to individually consider the displacement components. It is easy to verify that

$$\left(\boldsymbol{p}_{t,i}^b - \begin{bmatrix} 0 \\ 0 \\ r_{C,z} \end{bmatrix} \right) \times \begin{bmatrix} 0 \\ 0 \\ f_i \end{bmatrix} = \boldsymbol{p}_{t,i}^b \times \begin{bmatrix} 0 \\ 0 \\ f_i \end{bmatrix} \quad \forall\, i$$

and thus the displacement along $\boldsymbol{z}_b$ of the center of gravity does not modify the moment contribution. A value $r_{C,x} \neq 0$ and $r_{C,y} \neq 0$ introduces *distortion* effects along the pitch and roll directions respectively. After few computations it holds

$$\begin{aligned} M &= l(f_1 - f_3) + r_{C,x}(f_1 + f_3), \\ K &= l(f_2 - f_4) + r_{C,y}(f_2 + f_4). \end{aligned}$$

It is finally possible to write the mapping from the angular velocities to the force-torque at the vehicle:

$$\begin{bmatrix} Z \\ K \\ M \\ N \end{bmatrix} = \boldsymbol{B}_v \begin{bmatrix} \omega_{t,1}^2 \\ \omega_{t,2}^2 \\ \omega_{t,3}^2 \\ \omega_{t,4}^2 \end{bmatrix} \tag{6}$$

with

$$\boldsymbol{B}_v = \begin{bmatrix} b & b & b & b \\ 0 & b(l + r_{C,y}) & 0 & -b(l - r_{C,y}) \\ b(l + r_{C,x}) & 0 & -b(l - r_{C,x}) & 0 \\ -d & d & -d & d \end{bmatrix}.$$

III. QUADROTOR ADAPTIVE CONTROL

The thrusters velocities may be assumed as the control input for the quadrotor control problem. The dynamics of the low level motor controller, in fact, can be typically neglected with respect to the vehicle dynamics; thus, we can assume $\boldsymbol{u} = \begin{bmatrix} \omega_{t,1}^2 & \omega_{t,2}^2 & \omega_{t,3}^2 & \omega_{t,4}^2 \end{bmatrix}^{\mathrm{T}}$. Since the controller will output the desired force $\begin{bmatrix} Z_c & K_c & M_c & N_c \end{bmatrix}^{\mathrm{T}}$ at the vehicle, the control input is computed by

$$\boldsymbol{u} = \boldsymbol{B}_v^{-1} \begin{bmatrix} Z_c \\ K_c \\ M_c \\ N_c \end{bmatrix} \tag{7}$$

where $\boldsymbol{B}_v^{-1} \in \mathbb{R}^{4 \times 4}$ is the inverse of (6)

$$\boldsymbol{B}_v^{-1} = \begin{bmatrix} \dfrac{l - r_{C,x}}{4bl} & 0 & \dfrac{1}{2bl} & -\dfrac{l - r_{C,x}}{4dl} \\ \dfrac{l - r_{C,y}}{4bl} & \dfrac{1}{2bl} & 0 & \dfrac{l - r_{C,y}}{4dl} \\ \dfrac{l + r_{C,x}}{4bl} & 0 & -\dfrac{1}{2bl} & -\dfrac{l + r_{C,x}}{4dl} \\ \dfrac{l + r_{C,y}}{4bl} & -\dfrac{1}{2bl} & 0 & \dfrac{l + r_{C,y}}{4dl} \end{bmatrix}.$$

It is interesting to evaluate what happens if the mapping from the desired forces to the thrusters velocities is computed with the *estimated* mapping ($\hat{\boldsymbol{r}}_C$), while the effective mapping is physically related to $\boldsymbol{r}_C$:

$$\begin{bmatrix} Z \\ K \\ M \\ N \end{bmatrix} = \boldsymbol{B}_v|_{\boldsymbol{r}_C}\, \boldsymbol{B}_v^{-1}|_{\hat{\boldsymbol{r}}_C} \begin{bmatrix} Z_c \\ K_c \\ M_c \\ N_c \end{bmatrix} \tag{8}$$

i.e.,

$$\begin{bmatrix} Z \\ K \\ M \\ N \end{bmatrix} = \begin{bmatrix} 1 & 0 & 0 & 0 \\ \dfrac{\tilde{r}_{C,y}}{2} & 1 & 0 & \dfrac{b\tilde{r}_{C,y}}{2d} \\ \dfrac{\tilde{r}_{C,x}}{2} & 0 & 1 & -\dfrac{b\tilde{r}_{C,x}}{2d} \\ 0 & 0 & 0 & 1 \end{bmatrix} \begin{bmatrix} Z_c \\ K_c \\ M_c \\ N_c \end{bmatrix} \tag{9}$$

where the terms non belonging to the unitary matrix represent a coupling effect that may arise if the center of mass is wrongly estimated or neglected. Also, force along $\boldsymbol{z}_b$ and moment around $\boldsymbol{z}_b$ are not affected by a wrong estimation of the center of mass and thus $Z = Z_c$ and $N = N_c$.

In the following, an adaptive control law for quadrotor position and yaw regulation will be developed by taking into account persistent external disturbances and unknown center of mass position. The assumption that the roll and pitch dynamics are faster than the position one is made. Figure 3 sketches the control loop.

A. Altitude control

Let define $\tilde{z} = z_d - z \in \mathbb{R}$, $s_z = \dot{\tilde{z}} + \lambda_z \tilde{z} \in \mathbb{R}$ with $\lambda_z > 0$ and $\tilde{\boldsymbol{\gamma}}_v = \boldsymbol{\gamma}_v - \hat{\boldsymbol{\gamma}}_v$ with the hat symbol denoting the estimate of the corresponding variable.

We consider a scalar Lyapunov candidate function $V > 0$:

$$V(s_z, \tilde{\boldsymbol{\gamma}}_v) = \frac{m}{2} s_z^2 + \frac{1}{2} \tilde{\boldsymbol{\gamma}}_v^{\mathrm{T}} \boldsymbol{K}_{\gamma,z} \tilde{\boldsymbol{\gamma}}_v$$
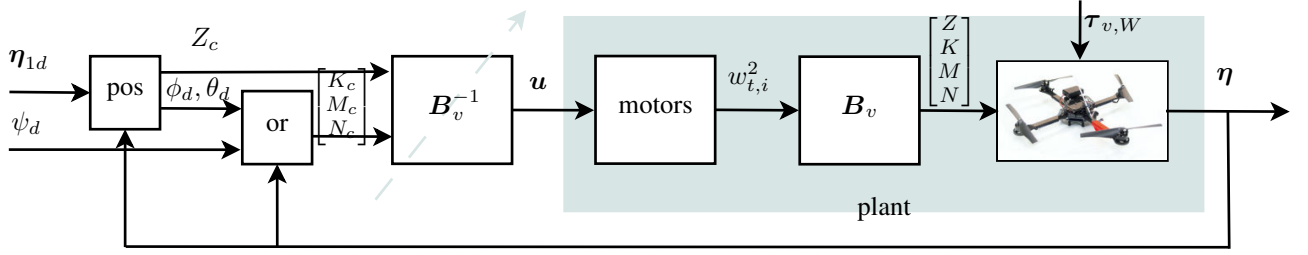
Fig. 3. Sketch of the control loop

whose time derivative is given by

$$
\begin{aligned}
\dot{V}(s_z, \tilde{\boldsymbol{\gamma}}_v) &= s_z \left(m\ddot{z}_d - m\ddot{z} + m\lambda_z \dot{\tilde{z}} \right) - \tilde{\boldsymbol{\gamma}}_v^{\mathrm{T}} \boldsymbol{K}_{\gamma,z} \dot{\hat{\boldsymbol{\gamma}}}_v \\
&= s_z \left(\boldsymbol{\phi}_z \boldsymbol{\gamma}_v - \cos\phi\cos\theta Z \right) - \tilde{\boldsymbol{\gamma}}_v^{\mathrm{T}} \boldsymbol{K}_{\gamma,z} \dot{\hat{\boldsymbol{\gamma}}}_v
\end{aligned}
$$

in which $\boldsymbol{\phi}_z$ dependency is $\boldsymbol{\phi}_z(\ddot{z}_d + \lambda_z \dot{\tilde{z}}, \dot{\boldsymbol{\eta}}, \boldsymbol{R}_I^B)$. $\dot{V}$ is made negative semidefinite by selecting

$$
\begin{aligned}
Z &= \frac{1}{\cos\phi\cos\theta} \left(\boldsymbol{\phi}_z \hat{\boldsymbol{\gamma}}_v + k_{pz} s_z \right) \\
\dot{\hat{\boldsymbol{\gamma}}}_v &= \boldsymbol{K}_{\gamma,z}^{-1} \boldsymbol{\phi}_z^{\mathrm{T}} s_z
\end{aligned}
$$

yielding

$$
\dot{V}(s_z, \tilde{\boldsymbol{\gamma}}_v) = -k_{p,z} s_z^2. \tag{10}
$$

We can now prove the system stability in a Lyapunov-like sense using Barbalats Lemma [20]. Since $V(s_z, \tilde{\boldsymbol{\gamma}}_v)$ is lower bounded, $\dot{V}(s_z, \tilde{\boldsymbol{\gamma}}_v) \leq 0$ and $\dot{V}(s_z, \tilde{\boldsymbol{\gamma}}_v)$ is uniformly continuous, then $\dot{V}(s_z, \tilde{\boldsymbol{\gamma}}_v) \to 0$ as $t \to \infty$ and thus $s_z \to 0$. As usual in adaptive control technique, we cannot prove asymptotic stability of the whole state, since $\tilde{\boldsymbol{\gamma}}_v$ is only guaranteed to be bounded.

It is interesting to implement a simpler version of the controller aimed at compensating the sole persistent dynamic terms, i.e., those terms preventing a null steady state error, yielding:

$$
\begin{aligned}
Z &= \frac{1}{\cos\phi\cos\theta} \left(\hat{\gamma}_z + k_{pz} s_z \right) \tag{11} \\
\dot{\hat{\gamma}}_z &= k_{\gamma,z}^{-1} s_z \tag{12}
\end{aligned}
$$

in which $\gamma_z \in \mathbb{R}$ embeds the joint contribution of the gravity and the vertical wind effects.

B. Horizontal position control

Let us recall the elementary rotation around z as

$$
\boldsymbol{R}_z = \begin{bmatrix} \cos(\psi) & \sin(\psi) \\ -\sin(\psi) & \cos(\psi) \end{bmatrix}
$$

and define as $\tilde{\boldsymbol{\eta}}_{xy} = \begin{bmatrix} x_d - x & y_d - y \end{bmatrix}^{\mathrm{T}} \in \mathbb{R}^2$ and $\boldsymbol{s}_{xy} = \dot{\tilde{\boldsymbol{\eta}}}_{xy} + \lambda_{xy} \tilde{\boldsymbol{\eta}}_{xy} \in \mathbb{R}^2$ with $\lambda_{xy} > 0$.

We consider a Lyapunov candidate function $V > 0$:

$$
V(\boldsymbol{s}_{xy}, \tilde{\boldsymbol{\gamma}}_v) = \frac{1}{2} m \boldsymbol{s}_{xy}^{\mathrm{T}} \boldsymbol{s}_{xy} + \frac{1}{2} \tilde{\boldsymbol{\gamma}}_v^{\mathrm{T}} \boldsymbol{K}_{\gamma,xy} \tilde{\boldsymbol{\gamma}}_v
$$

whose time derivative is given by

$$
\begin{aligned}
\dot{V} &= m \boldsymbol{s}_{xy}^{\mathrm{T}} \dot{\boldsymbol{s}}_{xy} - \tilde{\boldsymbol{\gamma}}_v^{\mathrm{T}} \boldsymbol{K}_{\gamma,xy} \dot{\hat{\boldsymbol{\gamma}}}_v \\
&= \boldsymbol{s}_{xy}^{\mathrm{T}} \left(m\ddot{\boldsymbol{\eta}}_{d,xy} - m\ddot{\boldsymbol{\eta}}_{xy} + m\lambda_{xy}\dot{\tilde{\boldsymbol{\eta}}}_{xy} \right) - \tilde{\boldsymbol{\gamma}}_v^{\mathrm{T}} \boldsymbol{K}_{\gamma,xy} \dot{\hat{\boldsymbol{\gamma}}}_v
\end{aligned}
$$

$$
= \boldsymbol{s}_{xy}^{\mathrm{T}} \left(\boldsymbol{\Phi}_{xy} \boldsymbol{\gamma}_v - Z \boldsymbol{R}_z^{\mathrm{T}} \begin{bmatrix} c_\phi s_\theta \\ -s_\phi \end{bmatrix} \right) - \tilde{\boldsymbol{\gamma}}_v^{\mathrm{T}} \boldsymbol{K}_{\gamma,xy} \hat{\boldsymbol{\gamma}}_v
$$

with $\boldsymbol{\Phi}_{xy}(\ddot{\boldsymbol{\eta}}_{d,xy} + \lambda_{xy}\dot{\tilde{\boldsymbol{\eta}}}_{xy}, \dot{\boldsymbol{\eta}}, \boldsymbol{R}_I^B) \in \mathbb{R}^{2\times16}$. This can be made negative semidefinite by selecting the *virtual* inputs ϕ and θ to solve

$$
\begin{aligned}
\begin{bmatrix} c_\phi s_\theta \\ -s_\phi \end{bmatrix} &= \frac{1}{Z} \boldsymbol{R}_z \left(\boldsymbol{\Phi}_{xy} \hat{\boldsymbol{\gamma}}_v + k_{p,xy} \boldsymbol{s}_{xy} \right), \\
\dot{\hat{\boldsymbol{\gamma}}}_v &= \boldsymbol{K}_{\gamma,xy}^{-1} \boldsymbol{\Phi}_{xy}^{\mathrm{T}} \boldsymbol{s}_{xy}.
\end{aligned}
$$

Notice that the necessity to integrate the dynamic parameters with two different adaptive laws for the horizontal and vertical controllers is consistent. Each estimate, in fact, is used for its respective controller. In both cases, Lyapunov theory implies boundedness, but not convergence to zero, of the errors. In case of persistent excitation, the two estimates should converge to the same values. Due to the lack of space, further discussion is out of the scope of this paper.

In this case too, by considering only the persistent dynamic terms, the controller reduces to a simple

$$
\begin{aligned}
\begin{bmatrix} c_\phi s_\theta \\ -s_\phi \end{bmatrix} &= \frac{1}{Z} \boldsymbol{R}_z \left(\hat{\boldsymbol{\gamma}}_{xy} + k_{p,xy} \boldsymbol{s}_{xy} \right) \tag{13} \\
\dot{\hat{\boldsymbol{\gamma}}}_{xy} &= k_{\gamma,xy}^{-1} \boldsymbol{s}_{xy} \tag{14}
\end{aligned}
$$

where $\hat{\boldsymbol{\gamma}}_{xy} \in \mathbb{R}^2$ represents the sole wind effect supposed constant in the inertial frame, and ϕ and θ can be easily computed yielding to ϕ_d and θ_d to be sent to the orientation controller.

C. Orientation control

The orientation control receives as input the desired roll, pitch and yaw; the formers are obtained by the position control equations. Notice that, in this case, it is necessary to explicitly consider the presence of a coupling effect among the desired and obtained forces as shown in eq. (8):

$$
\begin{aligned}
K &= K_c + \frac{\tilde{r}_{C,y}}{2} Z_c + \frac{b\tilde{r}_{C,y}}{2d} N_c, \\
M &= M_c + \frac{\tilde{r}_{C,x}}{2} Z_c - \frac{b\tilde{r}_{C,x}}{2d} N_c, \\
N &= N_c.
\end{aligned}
$$

It is worth noticing that neither the altitude nor the yaw control loop are affected by $\tilde{\boldsymbol{r}}_C$. The convergence to a steady state value for Z_c and N_c can thus be assumed, in addition, in absence of external moment disturbance along $\boldsymbol{z}_b$, at steady state $N_c = 0$. In any case, roll and pitch control can be

		simulated	initial estimate
mass	m	1.50 kg	1.49 kg
inertia	$\boldsymbol{I}_{Ob}$	$.025\boldsymbol{I}_3\,\text{kg m}^2$	not used in the reduced
length	l	30 cm	known
drag coeff.	b	1 Ns^2/rad^2	known
thrust coeff.	d	1 Nms^2/rad^2	known
center of mass	$\boldsymbol{r}_{C,b}$	$\begin{bmatrix}5 & 0 & 0\end{bmatrix}^\text{T}$ cm	$\begin{bmatrix}0 & 0 & 0\end{bmatrix}^\text{T}$ cm

TABLE I

DATA USED IN THE SIMULATION

λ_z	1.1	λ_{xy}	1.0	$k_{v,\phi\theta\psi}$	10.0
$k_{p,z}$	3.0	$k_{p,xy}$	2.0	$k_{p,\phi\theta\psi}$	40.0
$k_{\gamma,z}$	0.3	$k_{\gamma,xy}$	0.5	k_{rC}	5.0

TABLE II

GAINS USED IN THE SIMULATION

designed by considering the estimation error as an external, constant, disturbance:

$$K = K_c + \frac{1}{2}\left(Z_c + \frac{b}{d}N_c\right)\tilde{r}_{C,y}$$
$$M = M_c + \frac{1}{2}\left(Z_c - \frac{b}{d}N_c\right)\tilde{r}_{C,x}.$$

The disturbance value is unknown and its effect may be compensated by resorting to several adaptive control laws well known in the literature.

D. Center of mass estimation

In case a simple PD control is used for pitch and roll control the steady state error is experienced. This effect can be counteracted linking the roll-pitch error to a proper integral estimate of the center of mass position according to:

$$\begin{bmatrix}\dot{\hat{r}}_{C,x}\\\dot{\hat{r}}_{C,y}\end{bmatrix} = -k_{r_C}\begin{bmatrix}\theta_d - \theta\\\phi_d - \phi\end{bmatrix} \tag{15}$$

to be used in eq. (7).

IV. SIMULATIONS

Numerical simulations in a wide range of operative conditions have been run in order to verify the effectiveness of the proposed adaptive controller. Due to lack of space the sole reduced controller will be reported here with the aim to prove that the persistent terms have been effectively compensated resorting to a minimal set of dynamic parameters whose number is 5. The sampling time of sensors and controller has been set to $T = 1\,\text{ms}$; Tables I and II report the parameters used in simulation and, when applicable, the initial values used by the controller.

The simulation is run with a constant disturbance:

$$\boldsymbol{\gamma}_{v,W} = \begin{bmatrix}0.5 & 0.6 & 0 & 0 & 0 & 0\end{bmatrix}^\text{T}\quad[\text{N,Nm}]$$

and by requiring a regulation displacement of 1 m in the 3 directions x, y and z and 20 deg in yaw.

In the following, the controller will be compared with its non adaptive version; in the latter, despite the name, the sole altitude part of the controller will benefit from the adaptive action. Comparison with [16] is not possible since

the latter does not consider external disturbances, other than displacement of the center of mass that is not an *external* disturbance, and thruster mapping correction.

Figure 4 reports the norm of the position (top) and yaw (bottom) errors by applying the proposed control law (blue-solid line) and its non adaptive version (red-dashed line). As expected, the position error of the adaptive law goes to zero while the non adaptive version suffers from the presence of the external disturbance. Both the yaw errors goes to zero due to the mathematical properties of the quadrotor.
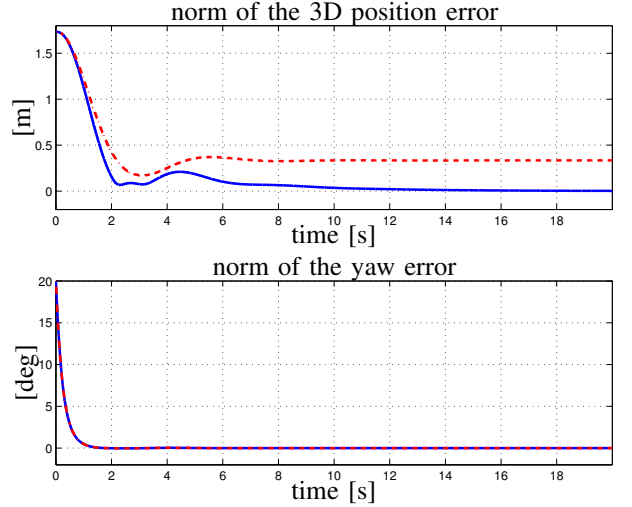
Fig. 4. Norm of the position (top) and yaw (bottom) errors by applying the proposed control law (blue-solid line) and its non adaptive version (red-dashed line)

Figure 5 reports the roll and pitch angles. On the top the desired (gray) and real (blue) values for the adaptive version while on the bottom the desired (gray dashed) and real (red dashed) values for the non adaptive simulation. Both controllers require a certain *inclination* at steady state to counteract for the wind.
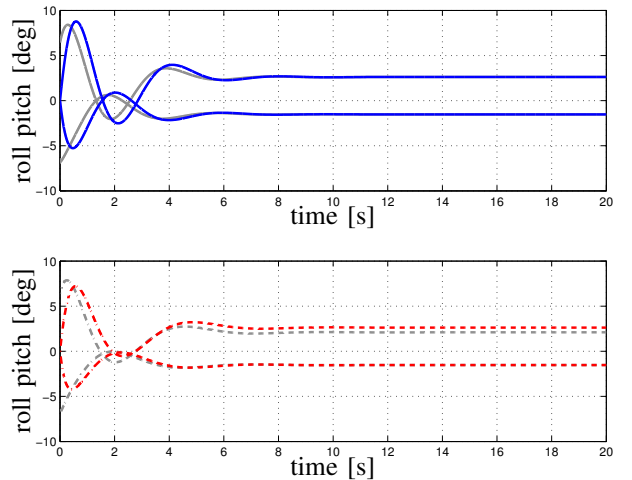
Fig. 5. Roll and pitch angle; on the top the desired (gray) and real (blue) values for the adaptive version while on the bottom the desired (gray dashed) and real (red dashed) values for the non adaptive simulation

Figure 6 reports the control effort in terms of force along z_b (top) and moments (bottom) for the first seconds with

(blue-solid line) and without (red-dashed line) adaptation. It can be noted that the values are almost the same; the improvement in the performance has not been achieved by an increased control effort but by a proper adapting action.
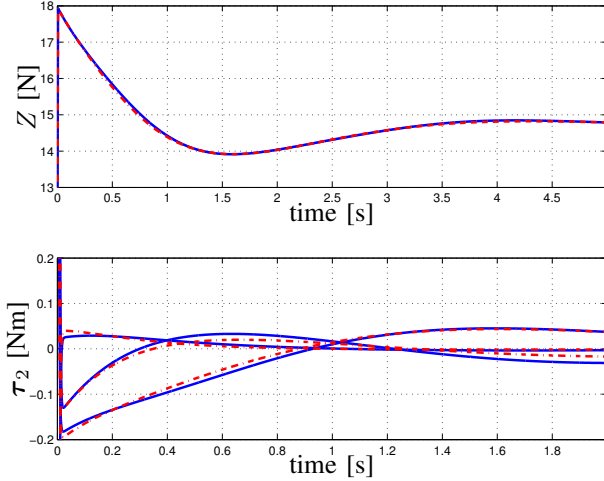

Fig. 6. Force along z_b (top) and moments (bottom) by applying the proposed control law (blue-solid line) and its non adaptive version (red-dashed line)

Figure 7, finally, reports the parameters used in the simulation (gray) together with the estimated one (blue). The steady state values is always the true one. This is due to the tautological persistent excitation arising when compensating for the sole persistent terms.
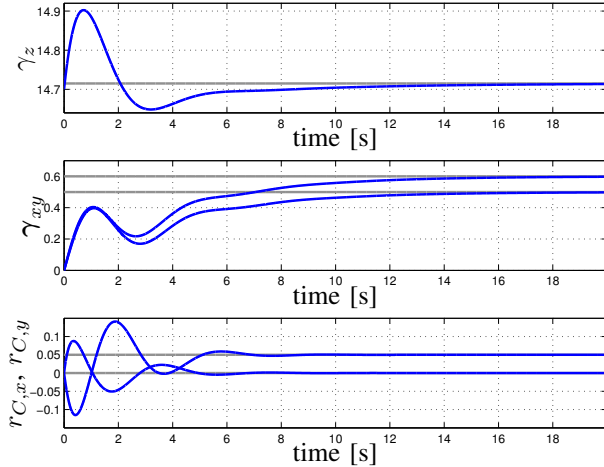

Fig. 7. Simulated parameters (gray) and estimated ones (blue)

V. CONCLUSIONS

Adaptive control for quadrotors is addressed in this paper. Convergence of the position and yaw error to zero is guaranteed in presence of constant external force/moment disturbance and unknown dynamic parameters, in particular for what concerns the center-of-mass position. A Lyapunov-based stability analysis has been used to design the controller, and results of numerical simulations are reported to validate it.

REFERENCES

[1] N. Michael, D. Mellinger, Q. Lindsey, and V. Kumar, "The GRASP multiple micro-UAV testbed," *Robotics and Automation Magazine*, vol. 17, no. 3, pp. 56–65, 2010.

[2] A. Franchi, C. Secchi, M. Ryll, H. H. Bülthoff, and P. Robuffo Giordano, "Bilateral shared control of multiple quadrotors," *Robotics and Automation Magazine*, vol. 19, no. 3, 2012.

[3] S. Weiss, D. Scaramuzza, and R. Siegwart, "Monocular-SLAM-based navigation for autonomous micro helicopters in GPS-denied environments," *Journal of Field Robotics*, vol. 28, no. 6, 2011.

[4] S. Shen, N. Michael, and V. Kumar, "Autonomous indoor 3D exploration with a micro-aerial vehicle," in *Proc. of the 2012 IEEE Int. Conf. on Robotics and Automation*, 2012.

[5] A. Bry, A. Bachrach, and N. Roy, "State estimation for aggressive flight in GPS-denied environments using onboard sensing," in *Proc. of the 2012 IEEE Int. Conf. on Robotics and Automation*, 2012.

[6] V. Grabe, H. H. Bülthoff, and P. Robuffo Giordano, "On-board velocity estimation and closed-loop control of a quadrotor UAV based on optical flow," in *Proc. of the 2012 IEEE Int. Conf. on Robotics and Automation*, 2012.

[7] J. Fink, N. Michael, S. Kim, and V. Kumar, "Planning and control for cooperative manipulation and transportation with aerial robots," *Int. Journal of Robotics Research*, vol. 30, no. 3, 2011.

[8] R. Spica, A. Franchi, G. Oriolo, H. H. Bülthoff, and P. Robuffo Giordano, "Aerial grasping of a moving target with a quadrotor UAV," in *Proc. of the 2012 IEEE/RSJ Int. Conf. on Intelligent Robots and Systems*, 2012.

[9] A. Franchi, C. Secchi, H. I. Son, H. H. Bülthoff, and P. Robuffo Giordano, "Bilateral teleoperation of groups of mobile robots with time-varying topology," *IEEE Transactions on Robotics*, 2012.

[10] A. Franchi, C. Secchi, M. Ryll, H. H. Bülthoff, and P. Robuffo Giordano, "Shared Control: Balancing Autonomy and Human Assistance with a Group of Quadrotor UAVs." *IEEE Robotics and Automation Magazine*, vol. 19, no. 3, pp. 57–68, 2012.

[11] P. Robuffo Giordano, A. Franchi, C. Secchi, and H. H. Bülthoff, "A Passivity-Based Decentralized Strategy for Generalized Connectivity Maintenance," *The International Journal of Robotics Research*, vol. 32, no. 3, pp. 299–323, 2013.

[12] P. Castillo, R. Lozano, and A. Dzul, "Stabilization of a mini rotorcraft with four rotors," *IEEE Control Systems Magazine*, vol. 25, no. 6, pp. 45–55, 2005.

[13] M.-D. Hua, T. Hamel, P. Morin, and C. Samson, "A control approach for thrust-propelled underactuated vehicles and its application to VTOL drones," *IEEE Transactions on Automatic Control*, vol. 54, no. 8, pp. 1837–1853, 2009.

[14] P. M. M. Fliess, J. Lévine and P. Rouchon, "Flatness and defect of nonlinear systems: Introductory theory and examples," *International Journal of Control*, vol. 61, no. 6, pp. 1327–1361, 1995.

[15] G. Antonelli, "On the use of adaptive/integral actions for 6-degrees-of-freedom control of autonomous underwater vehicles," *IEEE Journal of Oceanic Engineering*, vol. 32, no. 2, pp. 300–312, April 2007.

[16] I. Palunko, P. Cruz, and R. Fierro, "Agile load transportation. Safe and efficient load manipulation with aerial robots," *Robotics and Automation Magazine*, pp. 69–79, 2012.

[17] B. Siciliano, L. Sciavicco, L. Villani, and G. Oriolo, *Robotics: modelling, planning and control*. Springer Verlag, 2009.

[18] M. Gautier and W. Khalil, "Direct calculation of minimum set of inertial parameters of serial robots," *IEEE Transactions on Robotics and Automation*, vol. 6, pp. 368–373, 1990.

[19] G. Antonelli, F. Caccavale, and P. Chiacchio, "A systematic procedure for the identification of dynamic parameters of robot manipulators," *Robotica*, vol. 17, pp. 427–435, 1999.

[20] H. Khalil, *Nonlinear Systems*, 2nd ed. Upper Saddle River, New Jersey: Prentice-Hall, 1996.